Pergamon

Atmospheric Environment Vol. 32, No. 21, pp. 3679–3688, 1998

Printed in Great Britain

PII: S1352–2310(98)00091–0

1352–2310/98 $19.00 + 0.00

A MASS BALANCE METHOD FOR NON-INTRUSIVE MEASUREMENTS OF SURFACE-AIR TRACE GAS EXCHANGE

O. T. DENMEAD,*† L. A. HARPER,‡ J. R. FRENEY,§ D. W. T. GRIFFITH,¶ R. LEUNING† and R. R. SHARPE‡

† CSIRO Land and Water, GPO Box 1666, Canberra, ACT 2601, Australia; ‡ US Department of Agriculture, Agricultural Research Service, Watkinsville, GA 30677, U.S.A.; § CSIRO Division of Plant Industry, GPO Box 1600, Canberra, ACT 2601, Australia; and ¶ Department of Chemistry, University of Wollongong, Wollongong, NSW 2522, Australia

(*First received* 28 *August* 1997 *and in final form* 22 *February* 1998. *Published August* 1998)

Abstract—A mass balance method is described for calculating gas production from a surface or volume source in a small test plot from measurements of differences in the horizontal fluxes of the gas across upwind and downwind boundaries. It employs a square plot, 24 m × 24 m, with measurements of gas concentration at four heights (up to 3.5 m) along each of the four boundaries. Gas concentrations are multiplied by the appropriate vector winds to yield the horizontal fluxes at each height on each boundary. The difference between these fluxes integrated over downwind and upwind boundaries represents production. Illustrations of the method, which involve exchanges of methane and carbon dioxide, are drawn from experiments with landfills, pastures and grazing animals. Tests included calculation of recovery rates from known gas releases and comparisons with a conventional micrometeorological approach and a backward dispersion model. The method performed satisfactorily in all cases. Its sensitivity for measuring exchanges of CO_2, CH_4 and N_2O in various scenarios was examined. As employed by us, the mass balance method can suffer from errors arising from the large number of gas analyses required for a flux determination, and becomes unreliable when there are light winds and variable wind directions. On the other hand, it is non-disturbing, has a simple theoretical basis, is independent of atmospheric stability or the shape of the wind profile, and is appropriate for flux measurement in situations where conventional micrometeorological methods can not be used, e.g. for small plots, elevated point sources, and heterogeneous surface sources. © 1998 Published by Elsevier Science Ltd. All right reserved

Key word index: Dispersion, carbon dioxide, methane fluxes, emissions, landfills, animals.

INTRODUCTION

Micrometeorological methods are preferred for measuring fluxes of gases between the land surface and the atmosphere whenever their use is feasible because they do not interfere with processes of gas exchange in the natural environment and they integrate over large areas. Conventional micrometeorological techniques, however, require uniform, plane, surface sources and fetches long enough to ensure that horizontal concentration gradients are negligibly small. Typically, these fetch requirements impose lateral dimensions of hundreds of meters. Under these circumstances, the vertical flux density of the gas can be calculated from one-dimensional formulations, involving measurements at only one point in the air above the surface or involving measurements in only the vertical dimension. Eddy correlation and gradient diffusion methods are two such commonly-used approaches.

The large test areas required for application of conventional micrometeorological approaches and spatial variability in soil emission rates can present problems in many real-world situations where measurements of trace gas exchange are required. One example is the emission of gases from small, treated test plots, or from contaminated sites or landfills. Commonly, the emitting areas have lateral dimensions of tens rather than hundreds of meters and the source distribution is not uniform over the test area. Czepiel *et al.* (1996), for instance, report a coefficient of variation of 326% for 139 point measurements of methane emission from a landfill. In such circumstances, the measuring problem becomes two- or three-dimensional and conventional micrometeorological methods are inappropriate. An alternative approach is required. A second situation where an alternative approach is needed is the direct measurement of gas production from scattered point sources. Examples

* Author to whom correspondence should be addressed. Fax: + 61 6 246 5560; e-mail: tom.denmead@cbr.clw.csiro.au

are the production of methane by grazing animals and emissions of methane, nitrous oxide, or ammonia from animal dung and urine patches. In these instances, not only will there be non-uniform, temporally-varying source distributions, but the sources may be elevated also. Again, the problem becomes two- or three-dimensional.

Czepiel *et al.* (1996) have recently employed an alternative micrometeorological approach to measure the total CH_4 emission rate from a landfill. A tracer gas, SF_6, was released at a known rate at the landfill surface and the emission of CH_4 was calculated from the ratio of CH_4 concentration (above background) to SF_6 in the landfill plume at approximately 2 km downwind from the trailing edge.

Here we describe a mass-balance micrometeorological method which provides virtually no disturbance to gas production and emission processes and is suitable for use in small plots and where there are heterogeneous surface sources and elevated point sources. We illustrate its use by examples from experiments to measure methane and carbon dioxide emissions from a landfill and methane production by grazing cattle, and evaluate its performance through recovery tests and comparison with other micrometeorological approaches. Finally, its utility for measuring surface to air exchanges of CO_2, CH_4 and N_2O in various scenarios is examined.

METHODOLOGY

Theoretical

The mass balance method described here is an extension of one employed by Denmead *et al.* (1977) for measuring the emission of ammonia gas from a semi-infinite, treated strip. When gas is released from the ground into the atmosphere, it is convected horizontally by the wind while diffusing laterally and vertically. A rough rule of thumb which can be deduced from footprint analysis or numerical simulation, e.g. Wilson *et al.* (1982), is that the gas will be transported vertically to a height Z which is about 1/10 of the fetch.

The horizontal convective flux density at a point in the atmosphere is given by the product of horizontal wind speed u and gas density ρ_g.[1] If now, the gas is released within a defined space, the flux from the source can be calculated from the difference between the total gas fluxes across the upwind and downwind boundaries of the space. More specifically, if the gas is released within the confines of a square field of side X, as in the situation illustrated in Fig. 1a, then its mean emission rate $\bar{F}$ is given by

$$\bar{F} = \int_0^z \int_0^x \left[\bar{U}_z \left(\rho_{g_{4,z}} - \rho_{g_{2,z}} \right) + \bar{V}_z \left(\bar{\rho}_{g_{3,z}} - \bar{\rho}_{g_{1,z}} \right) \right] \mathrm{d}x \, \mathrm{d}z. \quad (1)$$

[1] The arguments here are in terms of gas density, but concentrations expressed in mixing ratios with respect to dry air, c, are used interchangeably in the paper. Following Webb *et al.* (1980), we note that $\rho_g = (m_g/m_a)\rho_a c$ where m_g and m_a are, respectively, the molecular masses of the gas and dry air and ρ_a is the density of dry air. $\rho_a = 0.348p/T$ where ρ_a is in kg m^{-3}, p is total barometric pressure in mb and T(K) is air temperature (List, 1951).

In equation (1) and in accordance with Fig. 1a, height is denoted by z, horizontal distance by x, boundary numbers by n ($n = 1$ to 4, with boundaries 1 and 2 upwind, 3 and 4 downwind), and the vector winds by U, normal to horizontal boundaries 2 and 4 and V, normal to boundaries 1 and 3. As well, time averages are denoted by an overbar. Thus, $\bar{\rho}_{4,z}$ denotes the time average at a height z on boundary 4.

It should be noted that the net horizontal flux density of gas, q, is the time mean of the product of the instantaneous wind speed u and gas density, i.e.

$$q = \overline{u\rho_g}. \quad (2)$$

If we represent u and ρ_g as the sums of the time means and deviations from those means, denoted by primes, then

$$q = \bar{u}\bar{\rho}_g + \overline{u'\rho'_g}. \quad (3)$$

The first term on the right-hand side of equation (3), i.e. the apparent convective flux, is the term that usually will be measured in applications of this technique. The last represents a turbulent, diffusive flux in the upwind direction, along the concentration gradient. If q is positive, $\overline{u'\rho'_g}$ is negative. Field tests by Leuning *et al.* (1985) suggest that the apparent horizontal flux, $\bar{u}\bar{\rho}_g$, overestimates the true flux by about 15%. Wind tunnel experiments by Raupach and Legg (1984) suggest 10%, while theoretical calculations by Wilson and Shum (1992), which account for cross-wind diffusion as well, suggest up to 20%. To calculate the production rates reported here, we have reduced the apparent convective fluxes, empirically, by 15%.

Sign conventions

Following the usual convention in meteorology, vector winds from the N and E are reckoned as being positive, and those from the S and W negative. The wind direction is specified by the angle Θ measured clockwise from N. Then,

$$U = u \cos \Theta \quad (4)$$

$$V = u \sin \Theta. \quad (5)$$

An import of gas to the test space is reckoned as being negative and an export as positive. With these conventions, $\bar{F}$ in equation (1) will be positive for gas production within the test space regardless of wind direction, and negative for gas consumption.

Test plot and gas sampling

We have employed a square test plot, 24 m × 24 m (Fig. 1a). For the applications described here, this plot size led to measurable concentration changes between upwind and downwind boundaries and a convenient maximum height of measurement (about 3 m). Gas concentrations were measured at four heights on each boundary. The selection of four heights was a compromise between the detail required in specifying the gas concentration profile and the time required to make a measurement of gas concentration on each air sample, in our case approximately 100 s. More sampling heights would enhance the precision of the flux measurement.

We employed measuring heights of 0.5, 1, 2 and 3.5 m. At each height on each boundary, horizontal sampling tubes extended along the complete 24 m. The tubes were 25 mm i.d. PVC pipe. In order to achieve even spatial sampling along the tube, 20 mm lengths of medical capillary tubing of 0.3 mm i.d. were inserted and sealed into the larger 25 mm tubing at 1 m intervals. The dimensions of the capillary tubing were such that at a total flow rate of 4 ℓ min^{-1} from each large sampling tube, the resistance to airflow across each capillary (calculated form Poiseuille flow) was > 100 times that along the length of the large tube, thus ensuring

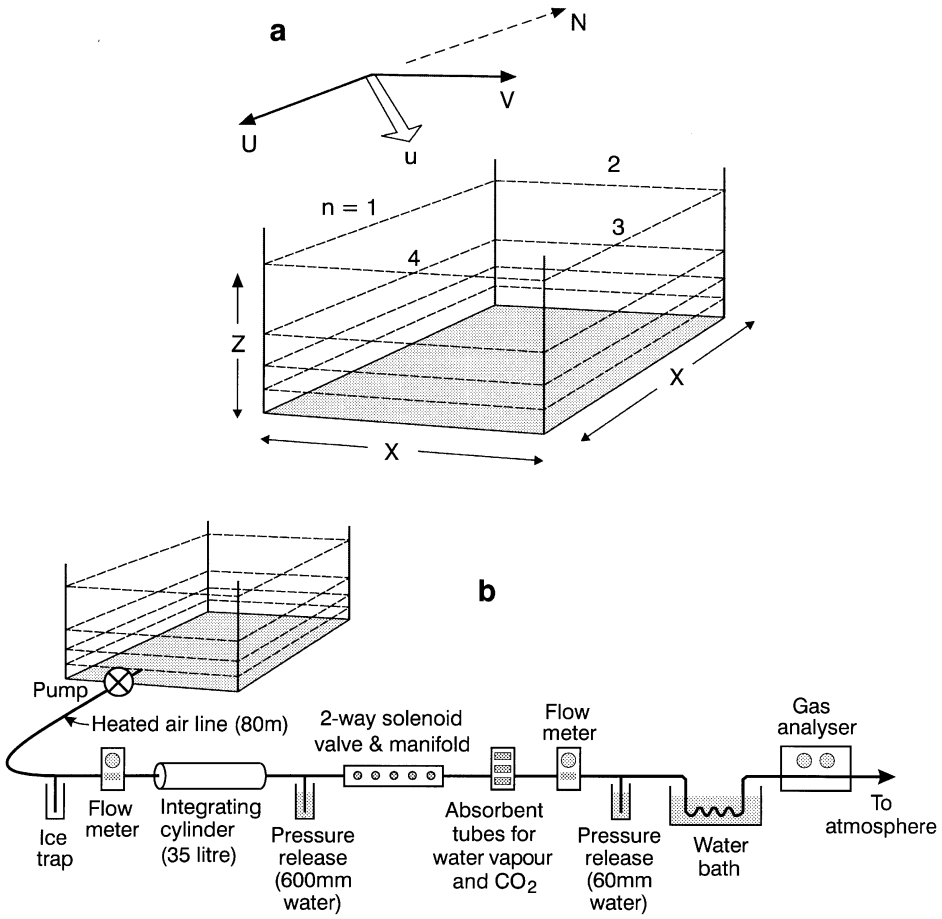

Fig. 1. (a) Schematic of experimental test plot and gas sampling array. In this case, side length X was 24 m and gas intakes were at heights of 0.5, 1, 2 and 3.5 m. u denotes total wind speed, U is the wind speed normal to N and S boundaries and V that normal to the E and W boundaries. (b) Schematic of analysis system.

negligible variation in intake along the latter's length. Tests of air flow, made by pumping air into one of the large sampling tubes and measuring the outflow of air through the capillary tubes along its length, confirmed equal flow rates through the capillaries within 5%.

In practice, each large tube was connected to a pump which then delivered the air under positive pressure through 80 m of heated 10 mm o.d. tubing to a mobile laboratory for measurement of its gas concentration on line. In our experiments, we have used, at various times, non-dispersive infrared (NDIR) gas analysers, a Fourier transform infrared spectrometer (FTIR), a tuneable diode laser (TDL) and a gas chromatograph (GC) for gas analysis. The measurements of CH_4 concentration reported in this paper were made with an ADC model 225 Mark II NDIR analyser and a Hewlett Packard Model 5730A GC with a flame ionisation detector, having resolutions of 0.2 and 0.1 ppmv, respectively, and those of CO_2 with a BINOS model BIN 1.2 Dual-Channel NDIR analyser with a differential resolution in this application of 0.3 ppmv.

Before analysis, the 16 air streams passed through ice traps to reduce their water vapour content, flow meters, and then integrating cylinders (with a volume of 35 ℓ) to damp out rapid changes in gas concentration (Fig. 1b). At the outlet end of the cylinder, most of the air was vented to the atmosphere through a water column 600 mm deep while the remaining air passed to a two-way solenoid valve which, when activated, allowed the air to pass into a manifold. Venting excess air through the water column ensured that air pressures and flow rates remained nearly constant for all air streams during analysis. When using NDIR and GC analysis, the manifold delivered air at 1.4 ℓ min^{-1} to a tube of magnesium perchlorate to remove residual water vapour (and for CH_4 analysis, Ascarite to remove CO_2), then a second flow meter. Finally, some of the manifold air was vented to the atmosphere through a water column 60 mm deep (to ensure absolute equality of pressure in all air streams) while the remaining air flowed through a copper coil in a water bath to remove temperature fluctuations and lastly, the gas analyser. Switching the solenoid valves and logging the analyser signals were computer controlled.

For CH_4 analysis by NDIR, the 16 air streams were compared with pure nitrogen as the reference gas. For CO_2 analysis, the reference gas was air from the top sampling level on the N boundary. In both cases, the reference gas was fed continuously through the reference cell of the NDIR analyser and the air streams or calibrating gases through the sample cell. The cycle for the sample cell consisted of reference gas, calibrating gas, and the 16 air samples, each switched at intervals of 100 s. With time for calculation, analysis and printing of the results, the cycle required 33 min for completion.

With the 15 ℓ volume of the airlines and the 35 ℓ of the integrating cylinders, the total buffering volume of the sampling system was 50 ℓ giving an approximate system time constant of 12.5 min. This was built into the system so as to guard against rapid changes in gas concentrations during the measurement cycle. Its disadvantage was that when wind

directions changed substantially, about 1 h was required for equilibrium to be established with the new concentration distribution.

Wind speed and direction

Small, sensitive cup anemometers (Casella) were used to measure total wind speeds at each of the sampling heights at two corners of the square. A fast-response, three-dimensional, propellor anemometer system (R.M. Young Associates) was used to measure the wind direction. The measurements of wind speed at each height $u_{z,i}$ and wind direction Θ_i in successive 50 s intervals during a measuring cycle or run were used to calculate the instantaneous vector winds $U_{z,i}$ and $V_{z,i}$ from equations (4) and (5). These were then averaged to produce the mean vector winds $\bar{U}_z$ and $\bar{V}_z$ for the run. The mean wind direction was calculated as $\tan^{-1}(\bar{V}/\bar{U})$ and the standard deviation of wind direction as $[-2\ln(\sqrt{\{\overline{\cos\Theta}^2 + \overline{\sin\Theta}^2\}})]^{1/2}$, where $\overline{\cos\Theta}$ and $\overline{\sin\Theta}$ are, respectively, the means of the $\cos\Theta_i$ and the $\sin\Theta_i$ for the run (Fisher, 1983).

Flux calculation

With the sampling system described above, equation (1) becomes

$$\bar{F} = X\int_0^z [\bar{U}_z(\langle\bar{\rho}_{g_{4,z}}\rangle - \langle\bar{\rho}_{g_{2,z}}\rangle) + \bar{V}_z(\langle\bar{\rho}_{g_{3,z}}\rangle - \langle\bar{\rho}_{g_{1,z}}\rangle)]\,dz, \quad (6)$$

where the angular brackets denote spatial averages. Equation (6) can be evaluated numerically using the trapezoidal rule.

Illustrative examples

Figure 2 shows mean methane concentration profiles measured in successive runs on the upwind and downwind boundaries of the test plot in two different experiments, full details of which will be given elsewhere. Figure 2a is derived from an investigation of methane production by cattle (Harper *et al*., 1998) and Fig. 2b from a study of methane emission from a landfill. In the first study, 4 cattle were grazed inside the test area. Wind speeds over the period represented in Fig. 2a were 2–3 m s^{-1} and the wind direction was steady at about 280°, just N of W. The mean rate of methane production by the four cattle at that time was 4.3 mg s^{-1}. Notable points are that, as expected, CH_4 concentrations on the upwind boundaries were nearly constant with height and close to the global, "clean-air", baseline value of 1.7 ppmv, but air on the downwind boundaries was generally richer in methane at lower heights, by up to 0.5 ppmv, and had virtually the same concentration as air upwind at the top sampling height of 3.5 m. This last point indicates that the sampling array was high enough to capture all the emitted gas. Another feature is that the profiles were not steady from run to run suggesting a fluctuating methane production rate, probably arising from alternating periods of feeding and ruminating by the cattle. Observations of animal activity during the experiment indicated that higher emissions occurred when the cattle were resting and ruminating than when they were grazing (Harper *et al*., 1998).

The concentration profiles at the landfill site, Fig. 2b, were obtained with winds of 5–7 m s^{-1} and wind directions of 288–300°. The mean rate of methane production in the test area at that time was 560 mg s^{-1}. Concentrations were very much higher than in the animal experiment, being as much as 30 ppmv at the lowest downwind sampling height. The concentration profiles on both the upwind boundaries (N and W) were very similar, but concentrations were well above baseline and not constant with height. This occurred because the test area was located within a much larger emitting area. With the wind from W, the fetch over the landfill was 75–100 m; hence, strong concentration profiles were already developed in the arriving air. Nonetheless, large and easily measurable concentration differences occurred across the test area, typically about 10 ppm between W and E boundaries at the bottom sampling height of 0.5 m. The precision required in concentration measurement in this situation was obviously very much less than in the animal experiment. Another difference is that the concentration profiles changed little from run to run, indicating a steady production rate.

Figure 3 illustrates the various steps in flux calculation. Figures 3a and b shows profiles of the horizontal flux density of methane corresponding to particular concentration profiles in Figs 2a and b where they are indicated by shading. The flux profiles represent the individual terms making up the integrand of equation (6) and the shaded area between them represents production. As expected from the wind directions, most of the methane produced in the test area was exported across the E boundary in both cases. However, most of the horizontal transport from the landfill occurred near the ground, whereas it was mostly between 0.5 and 2 m in the animal experiment. (The cattle belch methane and so constitute elevated point sources.) As indicated by the concentration profiles, the top sampling level was high enough to ensure that in both cases, most of the export of methane was accounted for. Figure 3c illustrates the time courses of the integrated methane flux across upwind and downwind boundaries in the cattle experiment, and the general dependence of the calculations on wind speed and direction. Methane export is represented by the shaded area in the figure. As noted previously, this increased and decreased depending on whether or not the animals were ruminating. Finally, Fig. 3d shows the corresponding production of CH_4 by the four cattle in the test plot, i.e. the $\bar{F}$ of equation (6).

Varying wind directions are the largest problem for this experimental approach. It is evident in Fig. 3c that as the wind direction swung from W to N, the main export boundary shifted from E to S. This resulted in large changes in the concentration profiles on all boundaries, but because of the long time constant of the sampling system, the new equilibrium profiles required about one hour to become established; hence the gap in the flux records. In our applications of the method, we have discarded runs in which the standard deviation of wind direction within the run exceeded 20°.

EXPERIMENTAL EVALUATION

Gas releases

Two series of tests have been conducted to evaluate the ability of the system to measure known rates of gas production.

Release of CH_4. Methane was released from a gas cylinder, through a flowmeter and airline at 20 mg s^{-1} from a point source at 0.5 m above ground in the centre of the test area. Releases were made on several days and were maintained for several hours on each day. As can be seen in Fig. 4, calculated recoveries were satisfactory only when wind speeds exceeded 2 m s^{-1}. The loss of flux for winds below 2 m s^{-1} is not surprising; anemometers can stall at low wind speeds and light winds are usually associated with variable wind directions which, as indicated above, also contribute to unreliability. In our experiments, we have discarded data when wind speeds at the top measuring height were < 2 m s^{-1}.

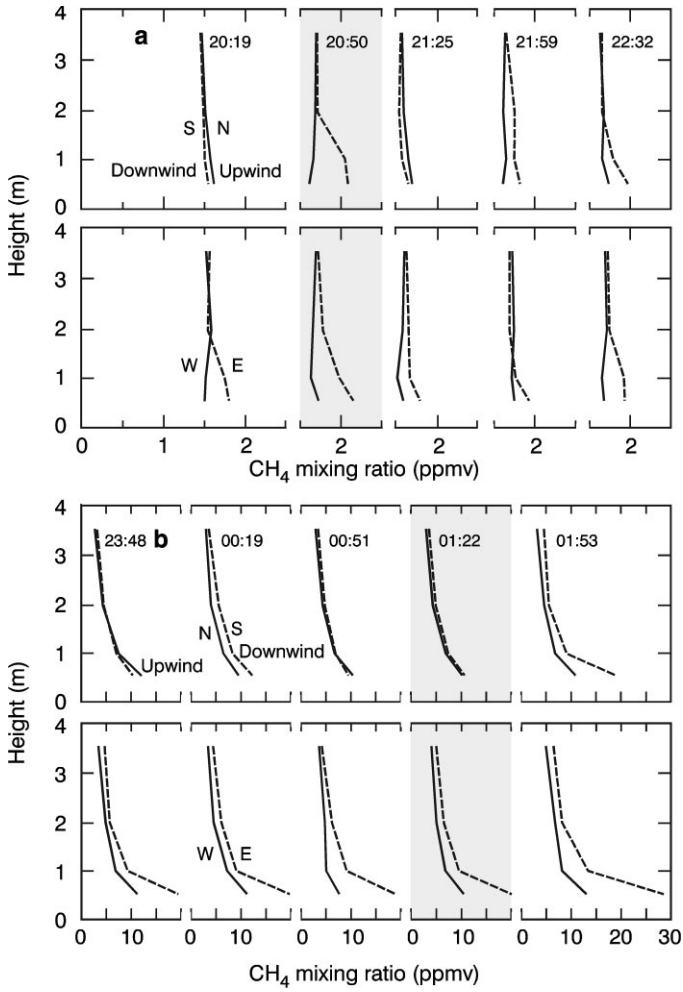

Fig. 2. Average CH_4 concentrations measured in consecutive runs during (a) the grazing experiment (when the mean wind speed was $2.3 \pm 0.3\,m\,s^{-1}$ and the mean wind direction $283 \pm 4°$), and (b) the landfill experiment (when the mean wind speed was $6.2 \pm 0.7\,m\,s^{-1}$ and the mean wind direction $293 \pm 5°$). Numbers to right of profiles denote starting times of the runs.

Release of CO_2. In this series, CO_2 was released in the same way as CH_4 from a point source in the test area at $165\,mg\,s^{-1}$. Recovery rates were more difficult to calculate than for the CH_4 releases because the test area was located in a large pasture which, through photosynthesis, constituted a significant CO_2 sink. It was thus necessary to account for the flux of CO_2 from atmosphere to pasture during the release in order to arrive at the true recovery rate. This was done by using the mass balance method to calculate the rate of consumption of CO_2 by the vegetation within the test plot for 1 h periods before and after the releases which were maintained for 1 h. The mean consumption rates of CO_2 before and after releases were added to the apparent rate of CO_2 production during the release period to calculate the CO_2 recovery. In another test, CO_2 was released at 1 m height at only 1 m W of the centre of the E boundary during westerly winds.

Recoveries during the 3 trials are given in Table 1. Recovery was excellent when releases were made at the plot centre, but some flux loss occurred when the release point was close to the downwind boundary. This loss is to be expected with only a limited number of sampling levels. Flux loss is more likely to be a problem in animal experiments where the sources are unrestrained. Obviously, more gas sampling levels are desirable in these experiments.

Comparison with a conventional micrometeorological method

As indicated in earlier sections, the test plot was located in a larger area of landfill in one experiment and pasture in the other. These circumstances provided opportunities to compare the mass balance flux calculations with fluxes calculated from a conventional micrometeorological approach based on aerodynamic relationships. These comparisons were not

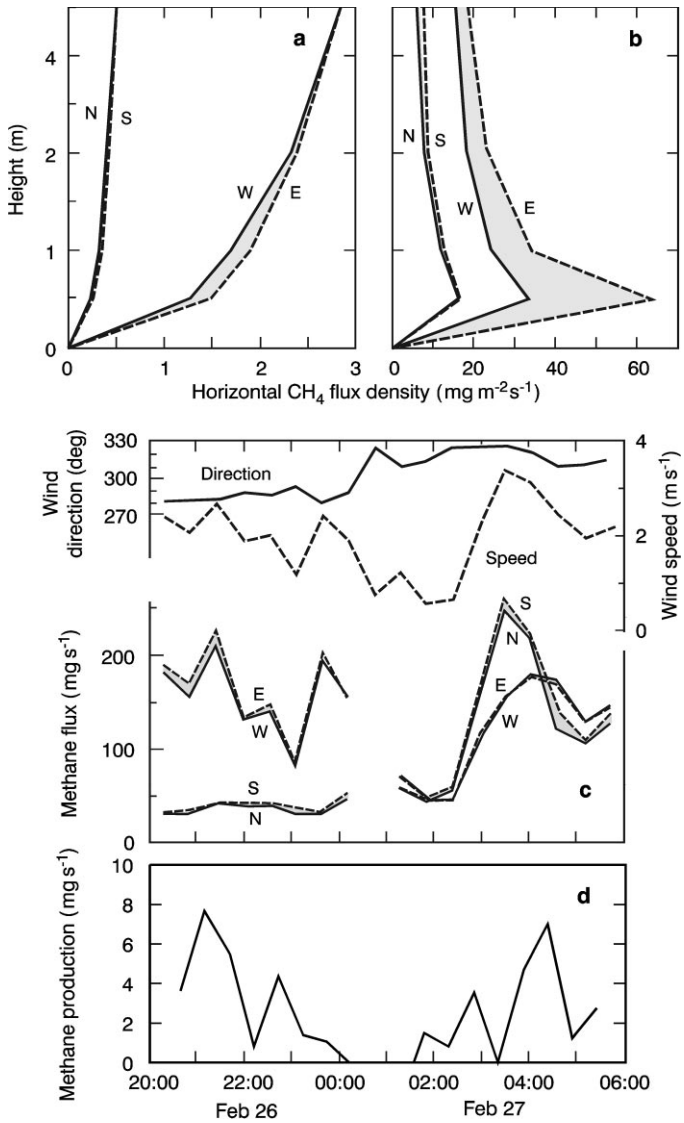

Fig. 3. Profiles of horizontal flux density of CH_4 on the boundaries of the test plot, which correspond to the concentration profiles shown in Fig. 2 at (a) 20:50 during the grazing experiment and (b) 01:22 in the landfill experiment. (c) Time course of the vertically integrated horizontal fluxes of CH_4 (to a height of 3.5 m) on the boundaries of the test plot during the grazing experiment and the corresponding wind speed at 3.5 m and the wind direction. The shaded areas represent the CH_4 export. The concentration profiles shown in Fig. 2a were measured in the first part of this period. (d) Corresponding time course of CH_4 production by the four cattle in the test plot, i.e. $\bar{F}$ in equation (6).

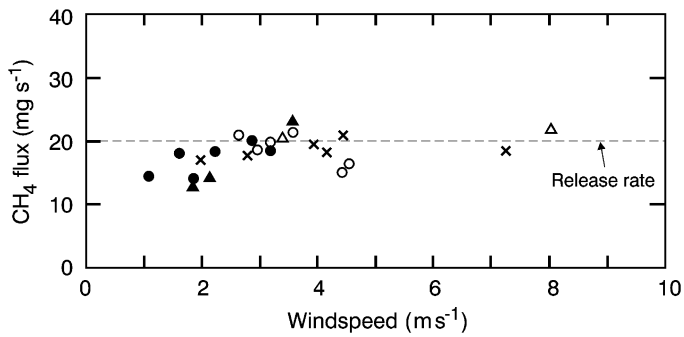

Fig. 4. Influence of wind speed on the recovery of CH_4 released at 20 mg s^{-1} at a height of 0.5 m at the plot centre. Different symbols represent different days.

Table 1. Recovery of released CO_2 in 3 trials

Main wind direction	E	E	W
Release point	[a]	[a]	[b]
Release rate ($mg\,s^{-1}$)	165	165	165
Mean of CO_2 consumption rates before and after release ($mg\,s^{-1}$)	137	108	80
Net CO_2 export rate ($mg\,s^{-1}$)	18	53	42
Recovery rate ($mg\,s^{-1}$)	155	161	122
Proportion recovered (%)	94	97	74

[a] 0.75 m high at plot centre.
[b] 1 m high at 1 m W of centre of E boundary.

so straightforward, however, because of the two dimensionality of the experimental situations. Substantial horizontal gradients in gas concentration were present in both landfill and pasture experiments. Of course, such gradients are the basis of the mass balance approach, but their influence on vertical gas transport needs to be accounted for in making the comparison.

The vertical flux density of a gas, Q, is described by

$$Q = -K_g \frac{\partial \rho_g}{\partial z} \tag{7}$$

where K_g is the eddy diffusivity for the gas (and scalars generally), which can be calculated from the wind profile and knowledge of atmospheric stability. Gas transport in two dimensions is described by

$$u \frac{\partial \rho_g}{\partial x} = \frac{\partial}{\partial z}\left(K_g \frac{\partial \rho_g}{\partial z} \right) \tag{8}$$

The term on the left-hand side of equation (8) is the horizontal transport due to advection, and that on the right-hand side is the divergence of the vertical flux. On integration, equation (8) gives

$$Q_0 - Q_z = \int_0^z u \frac{\partial \rho_z}{\partial x}\, dz \tag{9}$$

Q_0 and Q_z denoting, respectively, the vertical flux densities at the ground and at some height z. The mass balance method purports to measure Q_0, or rather AQ_0 (A being the area of the test plot), and the aerodynamic method calculates a Q_z. The longer the fetch, the smaller becomes the horizontal gradient of ρ_g, i.e. $\partial \rho_g / \partial x$, and the closer Q_z approaches Q_0. In our experiments with limited fetch, however, the term on the right-hand side of equation (9), representing flux divergence, is not trivial and cannot be ignored.

The aerodynamic flux Q_z was calculated from measurements of wind speed, gas concentration and temperature at heights of 0.5 and 1 m on the upwind boundary of the test plot, following procedures described by Thom (1975) and Paulson (1970). In conditions of neutral stability,

$$Q = \frac{k^2 (u_2 - u_1)\ (\bar{\rho}_{g,1} - \bar{\rho}_{g,2})}{[\ln(z_2/z_1)]^2} \tag{10}$$

where k is von Karman's constant and the subscripts 1 and 2 refer to the two measuring heights. In stable and unstable conditions, Eq. (10) carries some additional terms to account for the effects of thermal stratification on the diffusivities. The flux density calculated in this way is assumed to be the vertical flux density at the geometric mean of the two measuring heights, which in our case, is 0.7 m. It should be acknowledged that use of finite difference formulations like equation (10) in these circumstances may introduce some error into the estimate of Q_z because of the vertical flux divergence, but the error should not be too large because the measurement heights were close together.

The flux divergence between the surface and 0.7 m, the term on the right-hand side of equation (9), was calculated from the profiles of wind speed and gas concentration on the upwind and downwind boundaries of the test plot. (The comparison runs are drawn from periods when winds were essentially normal to a boundary of the test plot, thus simplifying the calculations.)

Comparisons for CH_4 emission from the landfill over a 10 h period are given in Fig. 5a. There was not one-to-one agreement, but, considering the assumptions made in calculating the aerodynamic fluxes and the large size of the flux divergence (about 40% of Q_0), the agreement is quite acceptable. For the 20 runs represented in Fig. 5a, the mean mass balance flux density (less 15% for back diffusion) was $0.98\,mg\,m^{-2}\,s^{-1}$ with a coefficient of variation (CV) of 32% and the mean of $[Q_{0.7} + \int_0^{0.7} (u \partial \rho_g / \partial x)\, dz]$ was $1.05\,mg\,m^{-2}\,s^{-1}$ with a CV of 16%.

A similar comparison for the pasture (with no animals present) is given in Fig. 5b. In this case the comparison is for gas consumption rather than production. The divergence term was smaller than for the landfill, amounting to 21% on average of the apparent surface flux. Again, there was not one-to-one agreement between the mass balance and the (corrected) aerodynamic fluxes, the ratio of the means of the two being 0.86. However, this could be expected since the pasture in the test plot was regenerating after being grazed heavily whereas the surrounding pasture was ungrazed. Both test plot and pasture exhibited the same diurnal trends and the same general dependence on solar radiation.

Comparison with a two dimensional dispersion model

Many dispersion models have been developed to relate surface fluxes to concentration profiles at specified distances downwind, e.g. Philip (1959), Wilson *et al.* (1982), and Flesch *et al.* (1995). We have made comparisons with predictions of the last model which is a backward Lagrangian stochastic model, referred to here as the LS model. In essence, it calculates trajectories of air parcels backward in time from the sensor location to the source. Its advantage is its simple input requirements. Computer-simulated gas releases are used to relate Q_0 to mean concentrations

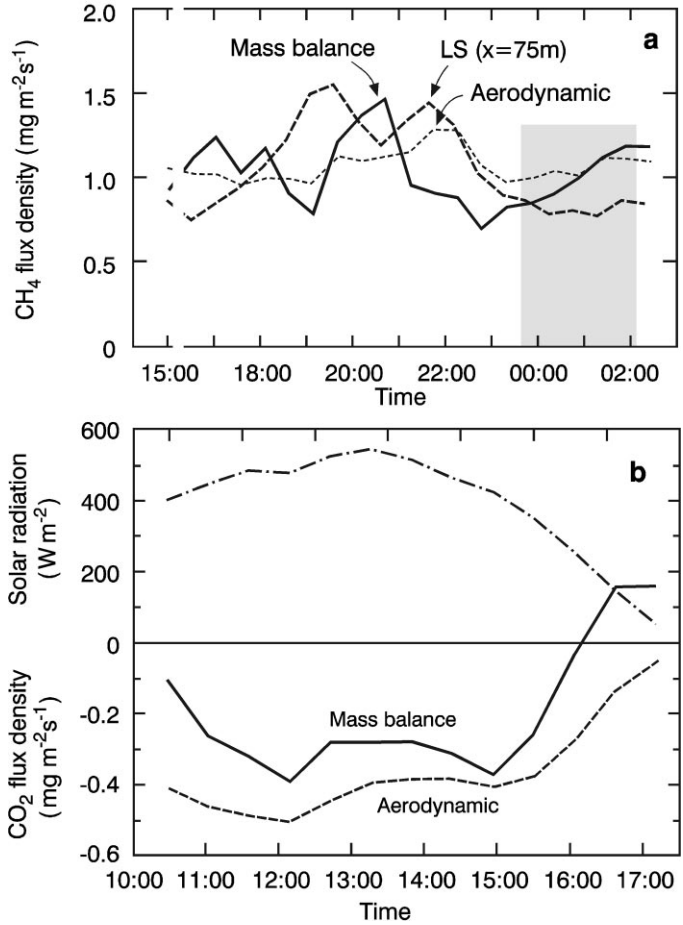

Fig. 5. (a) Comparison during the landfill experiment of vertical flux densities of CH_4 calculated for the test plot by the mass balance method, equation (6), and for the area upwind of the test plot by an aerodynamic flux-gradient technique, equations (7), (9) and (10) and the LS model of Flesch *et al.* (1995) equation (11). The concentration profiles shown in Fig. 2b were measured during the shaded interval. (b) Comparison of mass balance and aerodynamic measurements of CO_2 consumption by pasture.

developed at specified heights and distances downwind. The input information is the surface roughness z_0, the mean windspeed and the gas concentration (in excess of background) at *one* particular height and distance downwind, and the atmospheric stability. The output is Q_0. Solutions have the form

$$Q_0 = nu_z\rho_{g,z} \tag{11}$$

the coefficient n being calculated for the particular situation by the LS model.

Figure 5a presents comparisons of the mass balance methane flux density for the landfill with Q_0 calculated by the LS model of Flesch *et al.* (1995) from measurements at a height of 1 m on the upwind boundary. The calculations are for an essentially semi-infinite crosswind surface source, a fetch 75 m, neutral atmospheric stability and an assumed background concentration of 1.7 ppmv. As for comparisons with the aerodynamic fluxes, agreement is not perfect in the short term, but it is quite acceptable over periods of several hours. A more detailed comparison will be presented elsewhere, but the correct prediction of the mean flux and its general trend suggests both that the mass balance fluxes are in accordance with model expectations and that in some applications, the model might eventually prove a useful and simpler way to attack the flux estimation problem.

DISCUSSION

Despite operational problems caused by low wind speeds and changing wind directions, the mass balance method performed satisfactorily in the tests and applications described above. We have assessed its likely success in measuring trace gas emissions in other possible applications by simply scaling the results of the landfill and animal experiments for source strength and wind speed. The scaling exercise predicts likely concentration changes at 0.5 m between upwind and downwind boundaries of a 24 m × 24 m test plot

Table 2. Expected concentration difference between upwind and downwind boundaries of a 24 m × 24 m test plot at a height of 0.5 m for various emission scenarios

Gas	Source/sink	Production/consumption rate for test plot ($mg\ s^{-1}$)	Reference	Concentration difference (ppmv)
CO_2	Landfill	1200	Present study	13
CO_2	Wheat crop	500	Denmead and Raupach (1993)	5
CH_4	Landfill	600	This paper, Fig. 5a	15
CH_4	Rice crop	2	Yagi and Minami (1993)	0.1
CH_4	4 cattle	8	Johnson *et al.* (1994)	0.4
CH_4	60 sheep	10	Lockyer and Jarvis (1995)	0.5
N_2O	Landfill	10	F. Turatti, priv. comm. (1994)	0.1
N_2O	Fertilised grassland	0.05	Galle *et al.* (1994)	0.0005
N_2O	60 sheep	0.12	NGGIC (1996)	0.001

for various scenarios, based on published emission rates. It assumes a wind normal to one plot boundary with a speed of 3 $m\ s^{-1}$ at 3.5 m height. The expected concentration changes are listed in Table 2.

Table 2 suggests that the mass balance method can be used quite successfully to measure CO_2 uptake by vegetation. Concentration changes usually will be > 1 ppmv across the plot. With good technique, differences of 0.1 ppmv CO_2 can be measured routinely with NDIR analysers, for instance. The method might thus be useful in comparing CO_2 exchange rates of different crops growing side by side. It could prove useful also in FACE (free-air carbondioxide enrichment) experiments whose aim is to examine the effects of elevated CO_2 concentrations on plant functioning in the field. Provided measures were taken to damp out large concentration fluctuations, mass balance measurements within the enrichment zone could provide continuous, direct measurements of CO_2 exchange by the plants, which is needed information not presently obtained in FACE studies.

Table 2 indicates that for wetland or animal experiments, methane production would generate differences in CH_4 concentration across the test plot in the range 0.1–1 ppmv. If FTIR or TDL analysers with resolutions better than 0.01 ppmv are employed for concentration measurement, the method should have more than adequate sensitivity, but if NDIR or GC analysers are used, there will be occasions when the method is only just adequate. The resolutions of modern versions of these last instruments appears to be between 0.1 and 0.01 ppmv.

Use of the method to measure soil N_2O emissions from agricultural or natural sources will be more difficult. For these applications, a resolution better than 1 ppbv seems to be required. Very good experimental techniques will be needed to obtain this precision routinely under field conditions, even with FTIR and TDL analysers. Galle *et al.* (1994) suggest a measurement precision of 0.5 ppbv N_2O for FTIR and Hargreaves *et al.* (1994) indicate a precision of 0.14 ppbv for laboratory measurements with TDL, but suggest a lesser precision for field operations.

CONCLUSIONS

The main advantages of the mass balance method described here are:

1. like conventional micrometeorological approaches, the method is non-disturbing, but it requires fetches of only tens rather than hundreds of meters;
2. its theoretical and computational bases are simple;
3. it is appropriate for point sources and heterogeneous plane sources;
4. it does not require a particular form of the wind profile, and the calculations are independent of atmospheric stability.

The main disadvantages of the method include the following points:

(a) many gas analyses are required for one flux determination; 16 (or 8 differential) measurements would appear to be the minimum number; the time required can make the method cumbersome while the large number of measurements can introduce computational errors;
(b) the fluxes are calculated as residuals, differences between large numbers, which requires high-precision analytical techniques;
(c) consequent on the above points, temporal variability appears to be high, even when fluxes are supposedly steady in time;
(d) typical coefficients of variation in such circumstances are 20–30%;
(e) the method can be unreliable in light winds (say $< 2\ m\ s^{-1}$) and when wind directions are variable (say standard deviations $> 20^{\circ}$); some of the variability can also be attributed to the concentration measurement;
(f) in some applications, very high precision is required but newer gas analysers such as those employing FTIR and TDL offer promise for improved sensitivity.

Despite these difficulties, the mass balance method has considerable scope for trace gas flux measurement

in many situations where conventional micrometeorological methods cannot be used, e.g. for small plots, elevated point sources and heterogeneous surface sources. The development of new dispersion models such as the backward LS model of Flesch *et al.* (1995) may well lead to considerable simplifications of the mass balance technique, e.g. inference of the strength of *any* surface or volume source from one-point measurements at *any* location downstream.

Acknowledgements—We wish to acknowledge the technical support supplied by Alan Jackson, Mark Kitchen, Joselyn Moore, Fiona Ross and Barry Smith. We are particularly grateful to Fred Turatti for data on N_2O landfill emissions, and Tom Flesch for comparisons with the LS model. The landfill work received financial assistance from the Australian National Greenhouse Gas Inventory Committee.

REFERENCES

Czepiel, P. M., Mosher, B., Harriss, R. C., Shorter, J. H., McManus, J. B., Kolb, C. E., Allwine, E. and Lamb, B. K. (1996) Landfill methane emissions measured by enclosure and atmospheric tracer methods. *Journal of Geophysical Research* **101**, 16,711–16,719.

Denmead, O. T. and Raupach, M. R. (1993) Methods for measuring atmospheric gas transport in agricultural and forest systems. In *Agricultural Ecosystem Effects on Trace Gases and Global Climage Change*, eds by L. A. Harper, A. R. Mosier, J. M. Duxbury and D. E. Rolston, pp. 19–43. American Society of Agronomy Special Publication No.55, American Society of Agronomy, Madison.

Denmead, O. T., Simpson, J. R. and Freney, J. R. (1977) A direct field of measurement of ammonia emission after injection of anhydrous ammonia. *Soil Science Society of America Journal* **41**, 827–828.

Fisher, N. I. (1983) Comment on "A method for estimating the standard deviation of wind directions". *Journal of Climate and Applied Meteorology* **22**, 1971–1972.

Flesch, T. K., Wilson, J. D. and Yee, E. (1995) Backward-time Lagrangian stochastic dispersion models and their application to estimate gaseous emissions. *Journal of Applied Meteorology* **34**, 1320–1322.

Galle, B., Klemedtsson, L. and Griffith, D. W. (1994) Application of a Fourier transform IR system for measurements of N_2O fluxes using micrometeorological methods, an ultralarge chamber system, and conventional field chambers. *Journal of Geophysical Research* **99**, 16,575–16,583.

Hargreaves, K. J., Skiba, U., Fowler, D., Arah, J., Wienhold, F. G., Klemedtsson, L. and Galle, B. (1994) Measurement of nitrous oxide emission from fertilized grassland using micrometeorological techniques. *Journal of Geophysical Research* **99**, 16,569–16,574.

Harper, L. A., Denmead, O. T., Freney, J. R. and Byers, F. M. (1998) Direct measurements of methane emissions from grazing and feedlot cattle. *Journal of Animal Science* (submitted).

Johnson, K., Huyler, M., Westberg, H., Lamb, B. and Zimmerman, P. (1994) Measurement of methane emissions from ruminant livestock using a SF_6 tracer technique. *Environmental Science and Technology* **28**, 359–362.

Leuning, R., Freney, J. R., Denmead, O. T. and Simpson, J. R. (1985) A sampler for measuring atmospheric ammonia flux. *Atmoshperic Environment* **19**, 1117–1124.

List, R. J. (1951) *Smithsonian Meteorological Tables* (prepared by List, R. J.), pp. 527. Smithsonian Institution, Washington.

Lockyer, D. R. and Jarvis, S. C. (1995) The measurement of methane losses from grazing animals. *Environmental Pollution* **90**, 383–390.

NGGIC (1996) *Australian Methodology for the Estimation of Greenhouse Gas Emissions and Sinks*, *Workbook for Non-Carbon Dioxide Gases from the Biosphere* 5.1 1996. National Greenhouse Gas Inventory Committee, Department of the Environment, Sport and Territories,Commonwealth of Australia, Canberra.

Paulson, C. A. (1970) The mathematical representation of wind speed and temperature profiles in the unstable atmospheric surface layer. *Journal of Applied Meteorology* **9**, 857–861.

Philip, J. R. (1959) The theory of local advection: I. *Journal of Meteorology* **16**, 535–547.

Raupach, M. R. and Legg, B. J. (1984) The uses and limitations of flux-gradient relationships in micrometeorology. *Agricultural Water Management* **8**, 119–131.

Thom, A. S. (1975) Momentum, mass and heat exchange of plant communities. In *Vegetation and the Atmosphere*, ed J. L. Monteith, *Vol. 1*, pp. 57–109. Academic Press, London.

Webb, E. K., Pearman, G. I. and Leuning, R. (1980) Correction of flux measurements for density effects due to heat and water vapour transfer. *Quarterly Journal of the Royal Meteorologica Society* **106**, 85–100.

Wilson, J. D. and Shum, W. K. N. (1992) A re-examination of the integrated horizontal flux method for estimating volatilisation from circular plots. *Agricultural and Forest Meteorology* **57**, 281–295.

Wilson, J. D., Thurtell, G. W., Kidd, G. E. and Beauchamp, E. G. (1982) Estimation of the rate of gaseous mass transfer from a surface plot to the atmosphere. *Atmospheric Environment* **16**, 1861–1867.

Yagi, K. and Minami, K. (1993) Spatial and temporal variations of methane flux from a rice paddy field. In *Biogeochemistry of Global Change*: *Radiatively Active Trace Gases*, ed. R. S. Oremland, pp. 353–368. Chapman & Hall, New York.